We discuss here the effect of collisions. The electron-ion collision time for $T_e \simeq 10$ keV, $n = 10^{20}$ cm^{-3}, is approximately 1 ns. Hence in the absence of the baroclinic vector (driving force), the current and the magnetic field will die off rather quickly. However, the ion vorticity which can be dissipated only by the ion viscosity remains for a much longer period. The viscous damping rate for $k_\perp \rho_i > 1$ ($k_\perp^{-1}$ is the typical scale size) is given by $\nu_{ii}(k_\perp \rho_i)^{-1}$, where $\rho_i = v_{Ti}/\omega_{ci}$ is the ion gyroradius.[7] Hence for $T_i \simeq 10$ keV, $n = 10^{20}$ cm^{-3}, $B \simeq 1$ MG, we obtain the lifetime of the vorticity to be 10^2 ns.

Vortex formation in the laser-pellet interaction has several important implications: (1) If the vorticity is made large, the pellet may be destroyed as seen in curve 2 in Fig. 2; (2) ion transport is dominated by convection rather than by diffusion; and (3) the depleted density in the vortex core may produce channeling for the laser light leading to the enhanced transparency.

One of the authors (A.H.) would like to thank Professor K. Schindler and Professor G. Ecker for their hospitality during his stay at Ruhr University. This work is supported in part by Sonderforschungsbereich 162 Plasmaphysik Bochum/Jülich.

[1]J. A. Stamper *et al.*, Phys. Rev. Lett. 26, 1012 (1971).

[2]D. A. Tidman, Phys. Rev. Lett. 32, 1139 (1974).

[3]D. C. Colombant and N. K. Winsor, Phys. Rev. Lett. 38, 697 (1977); C. E. Max, W. M. Manheimer, and J. J. Thomson, Phys. Fluids 21, 128 (1978).

[4]A. Hasegawa and K. Mima, Phys. Fluids 21, 87 (1978).

[5]The choice of p_Θ^2 in the exponent can be generalized to $(p_\Theta - p^0)^2$ if there exists an average p_Θ. However, this choice simply shifts the value of eRA by p_0 in the result; p_0 does not play an essential role. If we choose p_Θ instead of p_Θ^2 in the exponent, the corresponding density becomes pinch type, i.e., $n \to 0$ as $R \to \infty$; see P. C. Clemmow and J. P. Dougherty, *Electrodynamics of Particles and Plasmas* (Addison Wesley, Reading, 1969), p. 242.

[6]R. E. Aamodt, Phys. Rev. Lett. 27, 135 (1971).

[7]A. A. Rukhadze and V. P. Silin, Usp. Fiz. Nauk. 96, 87 (1968) [Sov. Phys. Usp. 11, 659 (1969)].

Defect Annealing in Copper around Stage III

Th. Wichert, M. Deicher, O. Echt, and E. Recknagel
Fachbereich Physik, Universität Konstanz, 7750 Konstanz, Germany
(Received 1 November 1978)

Stage-III recovery in copper after electron and proton irradiation and after quenching is investigated by observation of perturbed $\gamma\gamma$ angular correlations. Two different types of intrinsic defects can be trapped at the radioactive impurities. The identity of the defects trapped after different damaging conditions proves that the recovery in stage III is mainly caused by two types of mobile defects, a monovacancy and a small vacancy complex, the latter being more mobile than the monovacancy.

We report on perturbed $\gamma\gamma$ angular correlation (DPAC) experiments in copper, which are the first unique proof that after quenching *and* irradiation the recovery in stage III (around 250 K) is caused by the mobilization of vacancies and that at least two different types of vacancies are mobile in this stage. Cu has been chosen as a prototype of those face-centered-cubic metals in which stages III and IV do not coincide. The information is obtained by comparison of the electric field gradients (efg) induced by defects which are trapped at the radioactive probe atoms in stage III after quenching—thus creating exclusively defects of vacancy type—and after low-dose electron irradiation—creating preferably isolated vacancies *and* interstitials (Frenkel pairs). Similar investigations in aluminum[1,2] could not contribute to the stage-III–stage-IV controversy, because here these stages do coincide.

Besides measurements of the defect-induced residual resistivity, rather microscopic techniques like positron annihilation or diffuse and small-angle x-ray scattering have been applied in order to understand the dynamics of the various lattice defects. They are well suited to study annealing of intrinsic defects (mainly $\Delta\rho$ measurements) or formation of new defect struc-

tures (microscopic methods). These methods, however, can hardly identify the types of defects which are thermally activated in a particular recovery stage, because only the *result* of defect migration is observed, whereas the migrating defects themselves remain invisible. So a twenty-year-old controversy still exists, whether recovery stage III in irradiated fcc metals has to be attributed to mobile monovacancies[3] or to self-interstitials in the dumbbell configuration.[4] Ample evidence has been claimed for both models,[5,6] but the arguments have been numerous rather than conclusive.

Recently radioactive tracer methods like Mössbauer effect[7] or time differential observation of the perturbed $\gamma\gamma$ angular correlation (DPAC)[8] have used the effect that intrinsic defects can be trapped at impurity atoms, if they are mobile and if a positive binding energy exists. The efg which these defects produce at their trapping center, i.e., a radioactive probe atom, can be precisely measured. So the method allows one to distinguish between different types of defects, even if several of them are simultaneously mobile. As in resistivity measurements, defect recovery is investigated in an isochronal annealing procedure, the annihilation probability of defects being replaced by the trapping probability at the probe atoms. But in contrast to $\Delta\rho$ measurements, the mobility of defects cannot be confused with the mobility of their antidefects.

Our investigation is divided into three parts: quenching and electron irradiation of pure Cu using less than 0.001-at.-ppm radioactive ^{111}In probe atoms, and H^+ irradiation of a dilute Cu alloy, containing additionally 10-ppm inactive In atoms. For the first two types of experiments the foils (50 μm thick, purity 99.999%) were doped by diffusing ^{111}In and tempered at 750 K in a vacuum better than 10^{-5} Torr. For the quenching experiments an apparatus as described by Lengeler[9] has been used: The foils are heated up to 1220 K in CO, dropped into dilute hydrochloric acid, kept at 220 K, and rapidly transferred to liquid nitrogen. In the second experiment the foils were irradiated at 4.2 K with 3-MeV electrons at the Institut für Festkörperforschung der Kernforschungsanlage, Jülich, to resistivity increases of 16 nΩ cm and 113 nΩ cm, corresponding to Frenkel-pair concentrations of 80 and 565 ppm, respectively.[10] For the third experiment the copper-indium alloy was doped at 300 K with ^{111}In at our 350-kV ion implantor and completely annealed. Then the foil was irradiated at 80 K with 300-keV H^+ to a dose of 4×10^{15} H^+/cm^2 or 120-ppm Frenkel pairs. The defect recovery has been studied in an isochronal annealing sequence in a liquid-nitrogen cryostat. For each step, the foils were pulled into a preheated oven and kept at the annealing temperature T_A for ten minutes, then a DPAC spectrum was recorded at 77 K.

In the DPAC experiment the radioactive probe atoms ^{111}In (half-life $T_{1/2}=2.8$ days) have to trap the migrating defects. The efg induced at the probes by these defects is measured at the isomeric nuclear state of the daughter nuclei ^{111}Cd ($T_{1/2}=84.5$ ns, spin $I=\frac{5}{2}$, quadrupole moment $eQ=0.74$ b). If a fraction B ($0\leq B\leq 100\%$) of all probe atoms is exposed to a nonvanishing field gradient eq, one obtains, after elimination of the exponential decay, the $\gamma\gamma$ correlation[11]

$$W(\theta,t)=1+A_2[(1-B)+BG_2(t)]P_2(\cos\theta) \qquad (1)$$

with

$$G_2(t)=\textstyle\sum_n s_{2n}\cos(nc\nu_Q t).$$

(For ^{111}Cd we have $c=3\pi/10$ and $A_2=-0.18$; the coefficients s_{2n} are tabulated.) The shape of the perturbation function $G_2(t)$ is clearly dominated by the quadrupole constant $\nu_Q=eQ\cdot eq/h$. Experimentally, we used a four-detector setup with detectors enclosing angles of $\theta=180°$ and 90°, respectively. The correlation function was extracted from the data by combining four simultaneously measured spectra to one "DPAC spectrum" $R(t)=W(180°,t)-1$. Further information on the method and the experimental setup is given in Ref. 11.

DPAC measurements on the samples after doping with ^{111}In ensure that the probe atoms are located in an unperturbed environment ($eq=0$), as expected for substitutional atoms in a well-tempered fcc lattice. Directly after quenching or irradiation the spectra do not show a periodic modulation, indicating that the defects are *statistically* distributed. Unique efg's do show up in the spectra after annealing above ~200 K. The number of ^{111}In atoms which have trapped defects during annealing reaches its maximum around $T_A=260$ K. In all experiments these In defect configurations disappear within a small temperature range around 300 K. In Fig. 1 DPAC spectra are shown which are measured on samples annealed at T_A after quenching, e^- irradiation with high and low dose, respectively, and H^+ irradiation. In all cases the spectra can be well fitted by Eq. (1) with two fractions B_1 and B_2 of

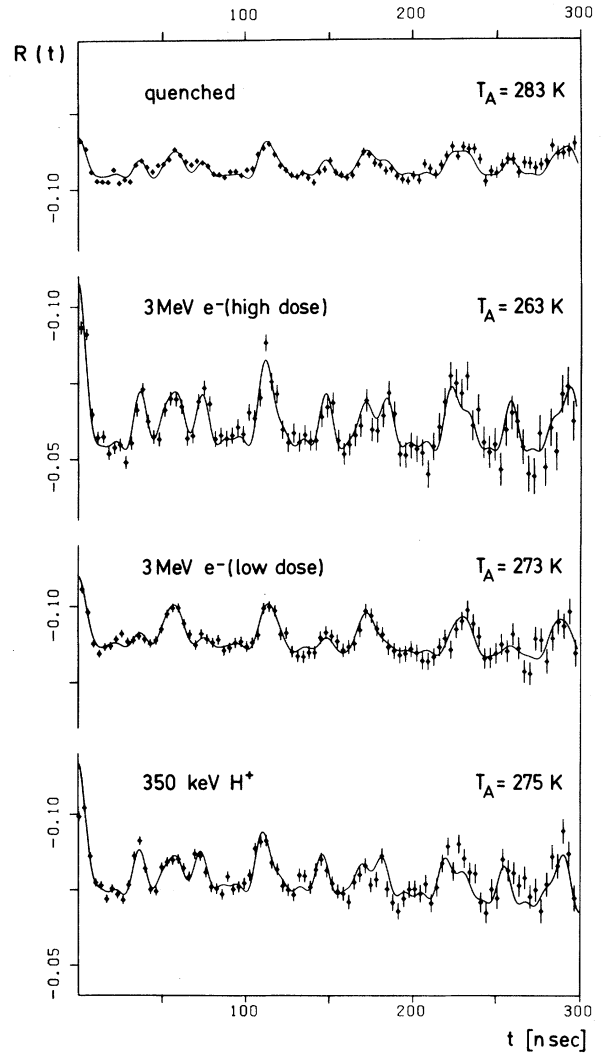

FIG. 1. DPAC spectra of ^{111}In in copper, as obtained after damaging by various procedures and annealing at a temperature T_A.

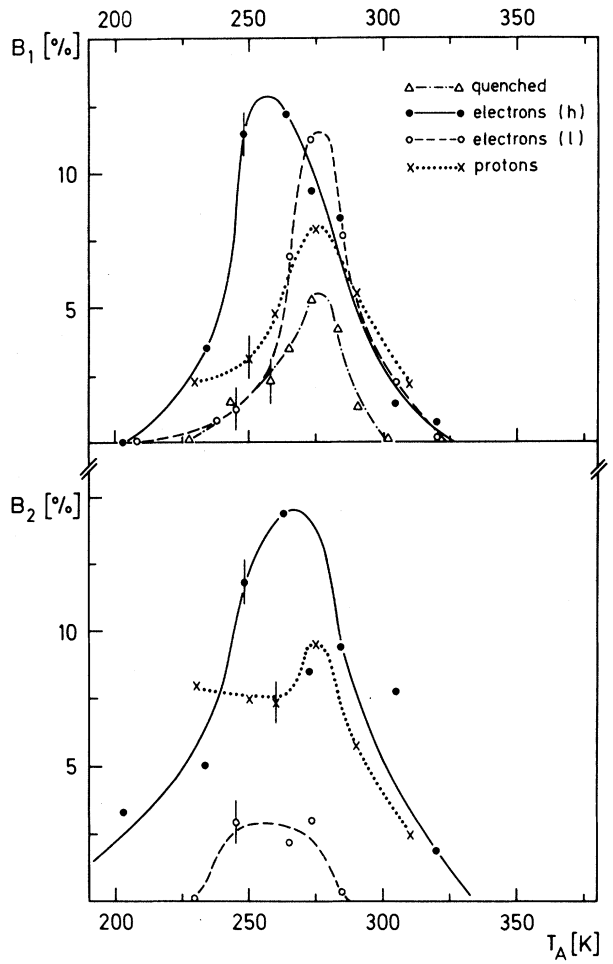

FIG. 2. Relative number B_i of ^{111}In probe atoms which have trapped defects of type ν_{Q1} (upper part) or ν_{Q2} (lower part), as a function of the annealing temperature T_A. (h) and (l) denote irradiation with high and low dose, respectively.

probe atoms influenced by unique efg's, corresponding to coupling constants ν_{Q_1} and ν_{Q_2}, respectively, and an unperturbed fraction $1-B_1-B_2$. The free parameters B_1, B_2, ν_{Q_1}, and ν_{Q_2} are obtained by least-squares fits to the spectra; the resulting theoretical functions are represented in Fig. 1 by solid lines.

The results of the three types of experiments can be summarized as follows.

(1) *Quenching.*—The coupling constants extracted from this experiment are $\nu_{Q_1}=117(2)$ MHz and $\nu_{Q_2}=181(2)$ MHz. The dependence of fraction B_1 on T_A is displayed in the upper part of Fig. 2 (dashed-dotted line); one clearly sees the trapping of one type of defect (characterized by ν_{Q_1}) in the temperature range 240 to 273 K. The trapping behavior of the second defect (characterized by ν_{Q_2}) has not been followed up completely; at 283 K the fraction B_2 of In atoms associated with this defect is 3.8%.

(2) *Electron irradiation.*—The coupling constants are $\nu_{Q_1}=116(1)$ MHz and $\nu_{Q_2}=181(1)$ MHz independent of the e^- dose. Figure 2 shows the formation probabilities B_1 (upper part) and B_2 (lower part) for high dose (solid line) and low dose (dashed line). The B_1 curve is significantly shifted to lower temperature for the sample with the higher defect concentration. The maximum value of B_2 shows a drastic dose dependence in contrast to B_1.

(3) *Proton irradiation.*—For the 10-ppm In alloy we have analyzed $\nu_{Q_1}=116(1)$ MHz and ν_{Q_2}

= 181(1) MHz. The maximum value of B_1 is found at 275 K (dotted line), similar to the behavior after low-dose e^- irradiation. B_2 reaches a plateau at 230 K and its maximum at 275 K.

The most important experimental result is that two different types of defects (uniquely characterized by ν_{Q1} and ν_{Q2}, respectively) are trapped at the impurity atoms during stage III, and that these defects are the same in the irradiated and the quenched samples, proved by the identity of the coupling constants extracted from the various experiments. Furthermore, both defect types must be *vacancylike*, as interstitiallike defects cannot be introduced into metals by quenching. In principle, the mobility of only one defect type would—via multiple trapping—suffice to create the two different defect configurations ν_{Q1} and ν_{Q2}. In our case, however, *two* types must be mobile: (i) Comparison of the e^- irradiations with high and low dose shows that fraction B_1 cannot be populated via B_2. (ii) The high-dose e^- irradiation and—more pronounced—the H^+ irradiation show that B_2 is formed prior to B_1 (around 200 K).

Electron irradiation preferably produces point defects in the copper matrix, and defect complexes mainly emerge from defect agglomeration at higher doses. The appearance of the two defect types after e^- irradiation, as displayed in the dependence of B_1 and B_2 on the annealing temperature T_A, can therefore be accounted for if one attributes ν_{Q1} to a monovacancy and ν_{Q2} to a divacancy or to another small vacancy complex: Fraction B_1 exhibits the second-order kinetics for trapping freely migrating vacancies, and B_2 is strongly suppressed in case of the low-dose irradiation. On the other hand, protons should produce relatively more small defect complexes than electrons; this is indeed reflected by the higher fraction B_2 as compared with B_1 in Fig. 2.

In an irradiated and subsequently annealed metal, the concentrations of vacancies and interstitials are nearly equal at the beginning of stage III. Therefore the trapping of any mobile vacancy (complex) at In atoms competes with its annihilation at interstitials. Assuming comparable trapping radii for both processes, one has to conclude that the concentration of the observed vacancies and vacancy complexes is so high that they significantly contribute to the total defect recovery in stage III. The somehow crude assumption concerning the trapping radii is fully justified by the H^+ irradiation of the Cu alloy: The probability for trapping mobile defects at ^{111}In is similar, although in these samples the concentration of In is 10^4 times larger than in the "pure" e^--irradiated samples. The assumption that ν_{Q1} and ν_{Q2} are *both* connected with vacancy complexes immediately leads to contradictory conclusions concerning the relative abundance of monovacancies and vacancy complexes in e^--irradiated metals.

From these results we conclude for copper, representing other fcc metals as well, the following: (i) Stage-III recovery in irradiated samples is mainly caused by mobile vacancylike defects. (ii) Monovacancies are mobile in stage III, far below stage IV. These statements are in clear contradiction to the two-interstitial model, which attributes stage-III recovery mainly to interstitials in the dumbbell configuration, assuming monovacancies to be immobile below stage IV. We further find for the first time that (iii) a second defect migrates in stage III. It is identified as a small vacancy complex (divacancy), which is more mobile than the monovacancy.

We acknowledge fruitful discussions with Dr. A. Weidinger, the technical assistance of Dr. S. Mantl, and financial support by the Bundesministerium für Forschung und Technologie.

[1]H. Rinneberg *et al.*, Phys. Lett. 66A, 57 (1978).
[2]H. Rinneberg *et al.*, Hyperfine Int. 4, 678 (1978).
[3]W. Schilling *et al.*, in *Proceedings of an International Conference on Fundamental Aspects of Radiation Damage in Metals, Gatlinburg, Tennessee, 1975*, CONF-751006 (National Technical Information Service, Springfield, Va., 1975), p. 470.
[4]A. Seeger, Ref. 3, p. 493.
[5]R. W. Balluffi, J. Nucl. Mat. 69 & 70, 240 (1978).
[6]R. Schindler, J. Nucl. Mat. 69 & 70, 331 (1978).
[7]W. Mansel *et al.*, Phys. Rev. Lett. 31, 359 (1973).
[8]C. Hohenemser *et al.*, Phys. Rev. B 11, 4522 (1975).
[9]B. Lengeler, Philos. Mag. 34, 259 (1976).
[10]P. Ehrhart *et al.*, J. Phys. F 4, 1575 (1974).
[11]O. Echt *et al.*, to be published.